Taylor & Francis
Taylor & Francis Group

Mechanics Based Design of Structures and Machines
An International Journal

ISSN: (Print) (Online) Journal homepage: https://www.tandfonline.com/loi/lmbd20

Seismic evaluation of the bridge with a hybrid system of cable and arch: Simultaneous effect of seismic hazard probabilities and vertical excitations

Salar Farahmand-Tabar & Majid Barghian

To cite this article: Salar Farahmand-Tabar & Majid Barghian (2023): Seismic evaluation of the bridge with a hybrid system of cable and arch: Simultaneous effect of seismic hazard probabilities and vertical excitations, Mechanics Based Design of Structures and Machines, DOI: 10.1080/15397734.2023.2172029

To link to this article: https://doi.org/10.1080/15397734.2023.2172029

Published online: 06 Feb 2023.

MECHANICS BASED DESIGN OF STRUCTURES AND MACHINES
https://doi.org/10.1080/15397734.2023.2172029

Seismic evaluation of the bridge with a hybrid system of cable and arch: Simultaneous effect of seismic hazard probabilities and vertical excitations

Salar Farahmand-Tabar and Majid Barghian

Department of Structural Engineering, Faculty of Civil Engineering, University of Tabriz, Tabriz, Iran

ABSTRACT

There are many parameters that affect the seismic behavior of the bridge, especially in the new type of bridges. In this research, the seismic behavior of a cable-arch bridge as a new type of bridge with a hybrid system of an arch and stay cables has been studied considering the effect of seismic hazard probabilities and vertical excitations. By considering these parameters, the seismic analysis was investigated in three steps: Response spectrum analysis to obtain general seismic behavior of the bridge, time-history analysis using seismic ground motion records to capture dynamic responses, and pushover analysis to determine the capacity of the bridge. The performance of the bridge was monitored, and the significance of considering seismic hazard probabilities and vertical excitations was investigated. Pointing out the effects of these parameters on the seismic behavior of the bridge, the results indicated a requirement for considering them to provide the seismic safety of the bridge.

ARTICLE HISTORY
Received 1 November 2021
Accepted 16 January 2023

KEYWORDS
Cable-arch bridge; seismic assessment; vertical excitation; seismic hazard probabilities

1. Introduction

Arch bridges are desirable for their economic feasibility and esthetic pleasure. However, among the other types of bridges, it has length limitations. The reason is that by increasing the arch span, the rise to span ratio becomes smaller, which may lead to the instability of the arch under different loads. The maximum span length for the arch bridge exists in Chaotianmen Bridge in China with only 552 m length, compared with the Suspension bridge of Akashi Kaikyo Bridge in Japan with the span of 1992 m and the cable-stayed bridge of Sutong in China with 1088 m span. To overcome this problem, some research studies have been done, and two hybrid bridges have been proposed. Klein and Yamout (2003) proposed the first system in which the bridge deck was supported by arches and stay cables. Regarding the stability of the arch ribs, the proposed system exhibited superior mechanical behavior compared to the conventional arch bridges (Nakamura et l. 2009). In 2002, the first bridge of this type was constructed in Malaysia, in which the arch ribs were concrete-filled steel tubes (CFST). In the second system, instead of anchoring stay cables on the bridge deck, they are anchored to the arch ribs. Modal analysis of this novel bridge concept was carried out by several researchers such as Zhao et al. (2005) and Luo et al. (2005). In 2007, the first real cable-stayed arch bridge, the Liancheng Bridge, was opened to traffic in China (Luo et al. 2005). Analytical and experimental investigation on the static and dynamic performance of the cable-arch prototype model bridge was carried out by Kang et al. (2013; 2014). Dynamic

CONTACT Salar Farahmand-Tabar farahmandsalar@gmail.com Department of Structural Engineering, Faculty of Civil Engineering, University of Tabriz, Tabriz, Iran.
Communicated by Wei-Chau Xie.

behavior of the cable-stayed arch bridge with CFST arch ribs under vehicle loading was conducted by Wang et al. (2015). The dynamic performance and response control of this bridge have been studied by Farahmand-Tabar and Barghian (2020) in different studies.

The investigation of extreme events such as the explosion or earthquakes is important for buildings and bridges (Farahmand-Tabar, Barghian, and Vahabzadeh 2019; Farahmand-Tabar and Barghian 2020; Aghabeigi and Farahmand-Tabar 2021). Investigating the seismic performance of a cable-arch bridge considering the hazard probabilities is essential for the safety assessment of the bridge. Meanwhile, several studies have been conducted to assess the seismic performance of the pure CFST arch bridges and cable-stayed bridges. As an example, the seismic response of a multi-span arch bridge was investigated by Li and Ge (2005). The seismic analysis of long and multi-span cable-stayed bridges was carried out by Jin et al. (2012) and He et al. (2009), respectively. The nonlinear seismic evaluation of a CFST arch bridge under seismic excitations was studied by Ma et al. (2011). The seismic assessment of the long-span cable-stayed bridge was carried out by Niu et al. (2014).

The seismic evaluations of bridge structures have been broadly investigated by researchers considering different parameters such as structural performance, bridge types, span length and type (straight or curved), different soil types, seismic risk, seismic safety, etc. In this regard, Dos Santos et al. (2019) investigated the vibration detection of a bridge with a curved deck using robotic total stations. Long and medium span bridges were investigated in different studies (Falamarz-Sheikhabadi and Zerva 2017; Marefat et al. 2019). Seismic fragility assessment of reinforced concrete bridges was investigated in few studies (Huang and Huang 2020; Taghinia et al. 2021; Todorov and Billah 2021).

Railway bridges are another kind of bridges which are dynamically required for an assessment (Yu et al. 2020; Liu et al. 2021; Zhang et al. 2021). Bridge pier and pile foundation as an important part of the bridge under seismic loading were studied (Cassese et al. 2020; Hao et al. 2017; Zheng et al. 2020). Earthquakes and seismic loads are probabilistic ones that each structure encounters within its lifetime. Therefore, the seismic risk probabilities are the crucial subjects on the seismic performance of the structures (Geradin et al. 2017).

On the other hand, research studies have proved that the vertical component of the earthquake excitation has a remarkable effect on the structures (Rahai 2004; Narayana and Patil 2015; Yang et al. 2016; Wang et al. 2016). In these investigations, the analysis results showed that the vertical excitation had a relatively large effect on the seismic performance of various structures, especially the bridge structures (Farahmand-Tabar and Barghian 2021).

To overcome the difficulties of the time-history analysis, the earthquake response spectrum can be used in the seismic assessment of the structure. An efficient response spectrum method for the analysis of structures under multi-support seismic excitations was proposed by Li and Li (2004) through introducing spectral parameters and correction factors which leads the analysis to obtain close agreement with results from Monte Carlo simulation and dramatic reduction of the computational time. To accomplish the response spectrum analysis of bridge structures, an engine-value problem should be solved to achieve the vibrational mode shapes and frequencies of the structure. For modal superposition analysis, Wang and Ye (2011) suggested that the minimum number of utilized modes can be accessed by computing the factors of cumulative effective mass. Then, the maximum response of each mode is calculated considering the design acceleration response spectrum charts chosen based on the bridge's site condition and the seismic design code. The total response of the structure is the suitable results combination of the modal response. An efficient strategy proposed (Bamer and Markert 2017) for response identification of nonlinear structures under nonstationary generated seismic excitations.

Considering the different methods and procedures for the seismic assessment of bridges, the new type of structures and bridges requires more detailed evaluations. The behavior of these structures, especially the hybrid long span bridges, are unknown and any parameter or loading

type can affect the overall behavior of the structure. Therefore, to generalize the design and construction of new types of structures, more parameters should be investigated. In this research, a full-scale finite element model of the cable-arch bridge (hybrid bridge in which the deck and arch of the bridge are supported by the cable system) is created, and the seismic response of the bridge is analyzed. The analysis is carried out using the response spectrum method to obtain general seismic behavior of the bridge, and the time history analysis to capture dynamic responses. In both cases, two hazard probabilities (10 and 3% exceeding probability in 100 years) is considered. Also, the effects of vertical seismic excitations are taken into account. Then, the pushover analysis is carried out on the isolated bridge piers to evaluate the capacity of the bridge. The main objective of this investigation is to study the seismic performance of the cable-stayed arch bridge as a new type of bridge with a hybrid system under seismic hazard probabilities and vertical seismic excitation to evaluate the safety of the bridge under extreme cases.

2. Liancheng bridge model

The cable-arch bridge model with the hybrid system of stay cables and an arch is illustrated in Figure 1a, b. The main and side span have 400 m and 120 m length, respectively, with 27 m width. The arch ribs include a rectangular cross-section made by six CFSTs (Figure 1c). The thickness of the steel tubes with a diameter of 85 cm alters from 2.0 to 2.8 cm regarding the position on the arch ribs. There are 11 wind bracings with pinned joints that stabilize both parallel arch ribs including: two rectangle connecting girders beneath the deck and two K-shaped wind bracings; Furthermore, one Ж-shaped bracing and six K-shaped bracings above the deck. All wind bracings are composed of steel pipe sections. The main span consists of a deck, transverse I-shaped girders, and longitudinal stringers. By using 39 hangers, the whole system is supported in two rows with an interval of 8 m. The stay cables are anchored on arch ribs and the deck with intervals of 8 and 10 m, respectively. The deck consists of lanes, expansion joints, pavements that have an influence on the seismic response of the bridge (Wei, Wang, et al. 2020).

According to Figure 2, the 3D finite element model of the whole bridge has been created in CSiBridge software. In the model, the fixed boundary conditions (in all degrees of freedom) are related to the ends of towers and the main and side arch ribs. The ends of two side spans were also fixed in all three translational directions, whereas the only permitted movement is the rotation along the lateral axis. Material properties regarding the structural elements, including the elasticity modulus, E, and cross-section area, A, are given in Table 1. The steel yield strength (f_y) and concrete compressive strength ($f_c^{'}$) are considered as 345 and 35 MPa, respectively. The element type used for cables is the cable element (tension-only bar element without the torsional/flexural stiffness). Cable sag and prestressing have been considered in cable models. Beam-column elements were used for towers and arches. For girders and bracings, beam and bar elements were utilized, respectively. The available data to verify the full-scaled modeling is the bridge mode shapes by Wang et al. (2015). So, ten mode shapes and their corresponding natural frequencies, as illustrated in Figure 3, were verified

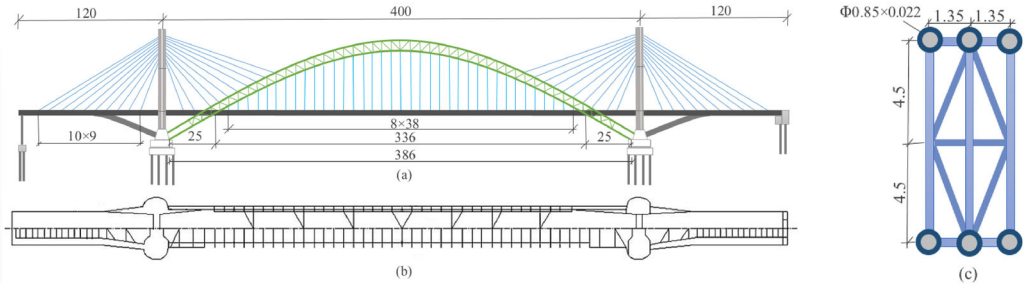

Figure 1. General view of the cable-arch bridge (values in meter): (a) elevation (b) Plan (c) cross-section of main arch rib.

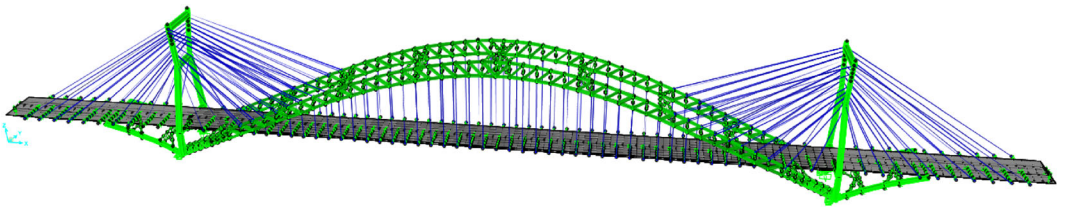

Figure 2. The cable-arch bridge model.

Table 1. Structural properties of bridge components (Wang et al. 2015).

Content	E (N/m^2)	A (m^2)	Element type	Material
Main arch rib (steel tube only)	2.1×10^{11}	1.430×10^{-3} (upper rib)	Beam-column	Steel
	2.1×10^{11}	1.304×10^{-3} (lower rib)		Steel
Bracing	2.1×10^{11}	4.128×10^{-3}	Bar	Steel
Hanger	2.05×10^{11}	2.117×10^{-3}	Cable	Steel
Cross girder	2.1×10^{11}	8.000×10^{-1}	Bar	Steel
Stay cable	1.95×10^{11}	4.340×10^{-3}	Cable	Steel
Main tower	3.5×10^{10}	1.143×10^{1} (upper tower)	Beam-column	Concrete
	3.5×10^{10}	1.074×10^{1} (middle tower)		Concrete
	3.5×10^{10}	1.304×10^{1} (lower tower)		Concrete
Arch rib of side span	3.5×10^{10}	8.800×10^{0}	Beam-column	Concrete

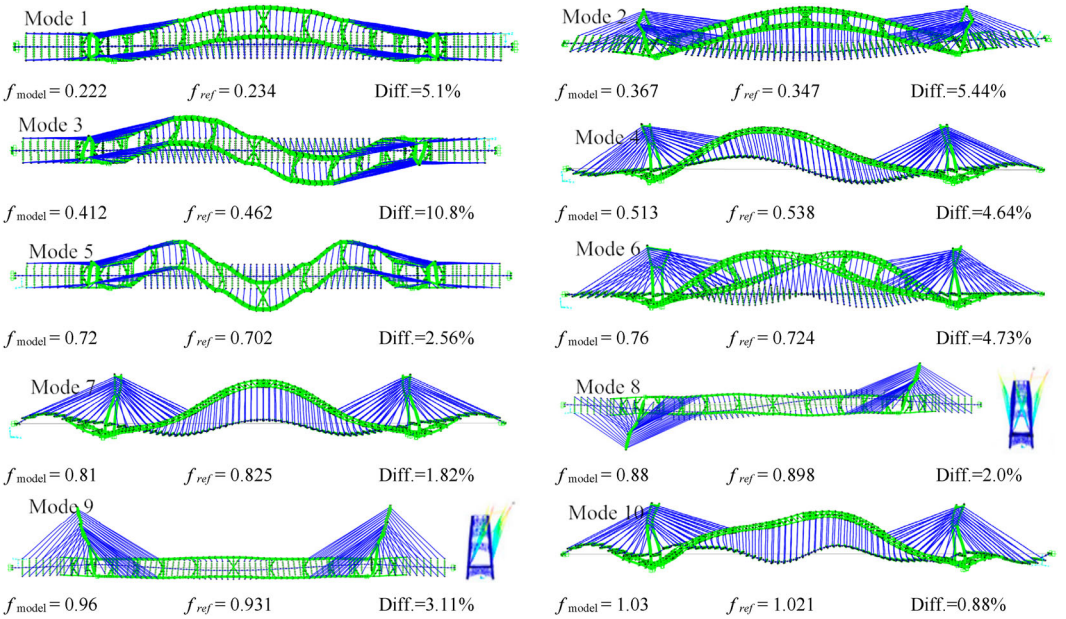

Figure 3. Verification of the cable-stayed arch bridge using mode shapes.

using the data given by Luo et al. (2005). The differences between the results are within 5%, which illustrates the reliability of the model. The assumed equivalent damping (Li et al. 2021) was 5%, and the applied analysis was modal time-history as a solution type with the time steps of 0.01.

3. Seismic evaluation of the bridge

The seismic evaluation of the cable-arch bridge is carried out in three steps: First, the three-component response spectrum is used to investigate the responses of different bridge components;

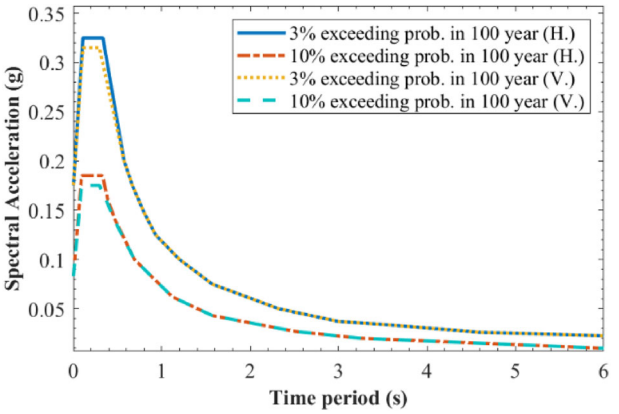

Figure 4. Target response spectra considering hazard probabilities: horizontal (H.) and vertical (V.) component.

Then, for precise evaluation, seismic ground motion records are used; Finally, the pushover analysis is carried out to evaluate the capacity of the bridge.

3.1. Response spectrum analysis

An actual time-history record is required to carry out the seismic analysis of a structure. However, it is not possible to have such records at every location. Also, the structural response depends on dynamic properties and the frequency content of the ground motion. So, the seismic analysis cannot be performed simply according to the Peak Ground Acceleration (PGA). To overcome these difficulties, the response spectrum can be used in seismic analysis of the structure. Using smooth design spectra has computational advantages to predict forces and displacements in structural systems. The spectra are applied to the structure according to the modal analysis of the bridge, considering the initial state of the bridge under its self-weight. According to bridge seismic design code (GB50011-2016) and considered site conditions of the bridge (soil type II), design acceleration response spectra under two probabilities are obtained. The peak accelerations of the two probabilities can be obtained through seismic risk evaluation which is the necessary procedure for the seismic design of long-span bridges. The horizontal and vertical spectra for both 3 and 10% exceeding probability (Figure 4) are utilized considering the combination rules recommended by seismic specifications of AASHTO (2012).

Appropriate mode combination methods should be utilized for the modal response combination since each mode obtains its maximum value at various moments. The square root of the sum of squares (SRSS) rules and the complete quadratic combination (CQC), which were derived based on the theory of random vibration, are the most commonly used rules for the combination of modes (Elnashai and Di Sarno 2008). The SRSS rule for mode combination is reliable when it is utilized to analyze moderate and small bridges which have sparse vibrational frequencies and a normal configuration. The SRSS method for structures with closely-spaced modes may underestimate or overestimate the actual response, depending on the resultant contributions effect of couple-modal terms, which can have both negative and positive signs. To combine the modal response of complex bridges such as suspension and cable-stayed bridges, the CQC rule of combination is more accurate, which was developed for stationary type and broadband input excitations using the correlation coefficient to consider the correlation of the modes.

3.2. Time history analysis using seismic ground motions

In the current study, various ground motion records were chosen as the input for seismic response analysis of the bridge. In this case, seven different earthquake records considering

Table 2. Selected ground motion records and their properties.

No.	Event name	Year	Station	Magnitude	Mechanism (Fault type)	Shear velocity (Vs30, m/s)	Epicentral distance (km)	Arias intensity (m/s)
01	Imperial Valley	1979	Niland Fire Sta.	6.53	Strike Slip	212.00	35.64	0.2
02	Darfield	2010	DORC	7.00	Strike Slip	280.26	29.96	0.2
03	Northridge	1994	San Jacinto-CDF	6.69	Reverse	306.76	147.47	0.1
04	Loma Prieta	1989	Salinas-John	6.93	Rev. Oblique	279.56	28.66	0.2
05	Kobe	1995	OSAJ	6.90	Strike Slip	256.00	21.35	0.2
06	Chichi	1999	CHY092	6.20	Strike Slip	253.72	33.02	0.1
07	Tabas	1978	Boshrooyeh	7.35	Reverse	324.57	24.07	0.3

intensities (Wei, Wang, et al. 2020) were selected from PEER strong ground motion databases (Table 2) in three orthogonal directions (longitudinal, lateral, and vertical). According to ASCE/SEI-7 (2016), if the analyzed records are the minimum of seven, the average of results is taken as the design values of engineering demand parameters (EDPs). All chosen records were matched to the considered spectrums utilizing the wavelets algorithm (Figure 5), which has been presented by Hancock et al. (2006) and used in the SeismoMatch Software. The parameters and corresponding values used for matching records are according to Table 3.

As shown in Figure 6, the ground motion records were matched to the spectra with different hazard probabilities. To logically model the structure subjected to the seismic load, all matched records were applied in three orthogonal directions.

3.3. Pushover analysis

For seismic analysis, pushover is considered a convenient assessment tool. So, the pushover analysis (continued from the initial state of dead load) was applied for each isolated bent-column in longitude and transverse directions while plastic hinge properties were assigned in advance. Therefore, the capacity curves of the bridge are achieved.

4. Results and discussion

The seismic loads (spectra with different hazard probabilities and seismic ground motion records matched to considered spectra) were applied to the structure in the horizontal and vertical direction. Responses corresponding to the mentioned load cases were compared with each other. Although the seismic loading was exerted on the structure at the end of the dead load case (simultaneous dead and seismic load), the seismic responses were compared with the responses of the dead load to evaluate the magnitude and the severity of the applied seismic loads. The displacement values of the bridge deck, arch, and towers under dead load are given in Table 4. Considering the symmetry of the model, the values for the half of the bridge deck are given. According to Table 4, the maximum vertical displacements of the bridge under dead load occurred in stations 36 and 240 m on the side and main deck with the values of 17.79 and 31.95 cm, respectively. The static responses of the bridge are given together with the seismic responses to be compared with each other.

4.1. Response spectrum analysis

4.1.1. Bridge arch

According to the seismic response analysis of the cable-arch bridge, the displacements of the main and side arches of the model are presented in Table 5. Under the seismic load case with the probability of 3%, the maximum lateral and vertical displacements exist in the middle and quarter

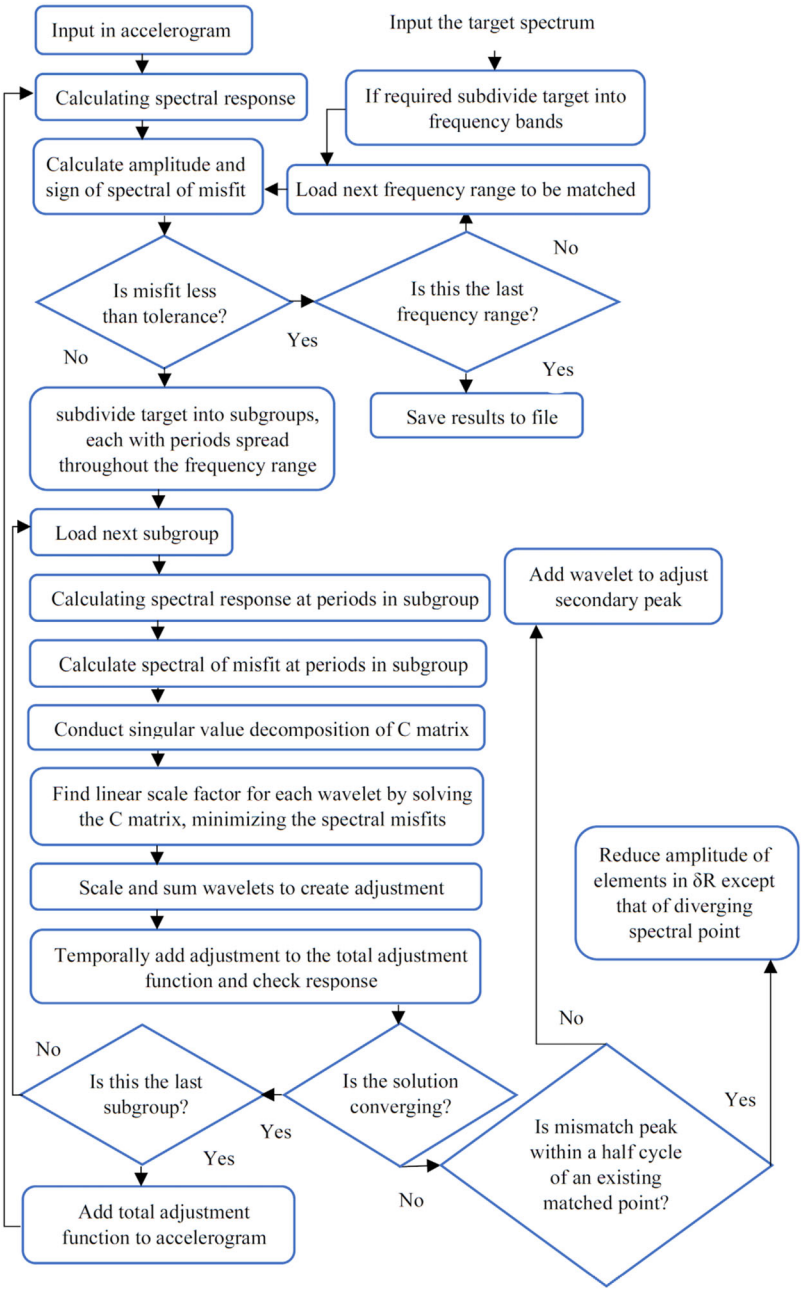

Figure 5. Algorithm for matching accelerograms to target response spectrum.

of the main deck, which is equal to 1.98 and 0.49 m, respectively. However, these responses for the side arch are equal to 0.04 and 0.13 m, respectively.

4.1.2. Hangers and stay-cables

The role of stay-cables in supporting the main arch is significant in this kind of bridge; because the longitudinal and lateral displacements of the arch are controlled by these cables, which lead to stability of the arch and the whole bridge. Therefore, the forces comparison of hangers and

Table 3. Values of the parameters used in SeismoMatch.

Parameters	Values
Mismatch tolerance	0.3
Max iteration	30
Scale factor	1
Min Eigen value	0.1
Max num. of waves	10
Additional waves	20
Off diagonal reduction	0.7
Group size	250

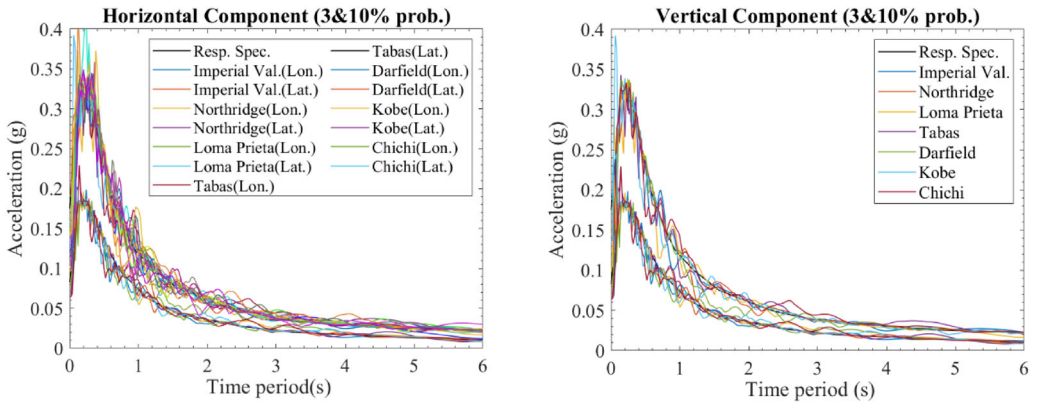

Figure 6. Response spectra and matched records.

Table 4. Displacement values of the bridge components under dead load.

		Displacement (cm)		
Bridge components	Stations (m)	Long.	Lat.	Vert.
Main Arch	Support (120)	0	0.00	0.00
	1/8 span (170)	6.81	0.50	−19.15
	1/4 span (220)	6.59	0.03	−26.75
	3/8 span (270)	1.82	0.03	−18.39
	Mid span (320)	0.001	0.01	−13.84
Side Arch	Mid span	0.2	0.02	1.03
	The vault	0.81	0.00	6.40
Towers	Bent columns	0.237	0.054	0.58
	Top of tower	11.56	0.254	2.10
Main deck	1/10 span (160)	0.59	16×10^{-06}	21.02
	3/8 span (240)	0.60	19×10^{-06}	31.95
	Mid span (320)	0.65	20×10^{-06}	23.61
Side deck	3/10 span (36)	0.59	2×10^{-06}	17.79
	Mid span (60)	0.82	5×10^{-06}	10.76
	Tower joint (120)	0.68	14×10^{-06}	1.91

stay-cables under various load cases are given in Figure 7. From these figures, the effects of the seismic load case with the probability of 3% are considerable among the other forces of hangers and stays. These effects also become severe when the vertical seismic excitation is considered in the seismic analysis of the bridge. The terms RS_{xy} and RS_{xyz} refer to the response spectrum load case of horizontal and three-component excitations, respectively.

4.1.3. Bridge deck

The structural responses such as displacements, forces, and moments diagrams under different load cases along the layout line are shown in Figure 8. Similar to previous results, the responses

Table 5. Displacements of the main and side arches under dead and seismic load cases.

	Longitudinal disp. (cm)			Lateral disp. (cm)			Vertical disp. (cm)		
		Response Spec.-XY			Response Spec.-XY			Response Spec.-XY	
Locations on the bridge	Dead load	(P. 10%)	(P. 3%)	Dead load	(P. 10%)	(P. 3%)	Dead load	(P. 10%)	(P. 3%)
Main arch support (120 m)	0	0	0	0	0	0	0	0	0
1/8 span of main arch (170 m)	6.81	10.06	12.35	0.50	−23.14	−39.52	−19.15	−25.48	−29.90
1/4 span of main arch (220 m)	6.59	12.42	16.51	0.03	−62.85	−107.84	−26.75	−39.81	−48.97
3/8 span of main arch (270 m)	1.82	6.03	8.99	0.03	−99.20	−169.89	−18.39	−28.80	−36.12
1/2 span of main arch (320 m)	0.001	2.69	4.59	0.01	−115.27	−197.52	−13.84	−17.54	−20.20
5/8 span of main arch (370 m)	−1.82	6.03	−9.00	0.03	−99.18	−169.85	−18.39	−28.78	−36.08
3/4 span of main arch (420 m)	−6.59	12.44	−16.55	0.03	−62.82	−107.77	−26.75	−39.88	−49.09
Side arch support	0	0	0	0	0	0	0	0	0
1/2 span of side arch	0.20	1.04	1.58	0.02	1.52	2.50	−1.03	−2.90	−4.10
The vault of side arch	−0.81	−2.07	−2.88	0	−2.43	−4.02	−6.40	−10.53	−13.39

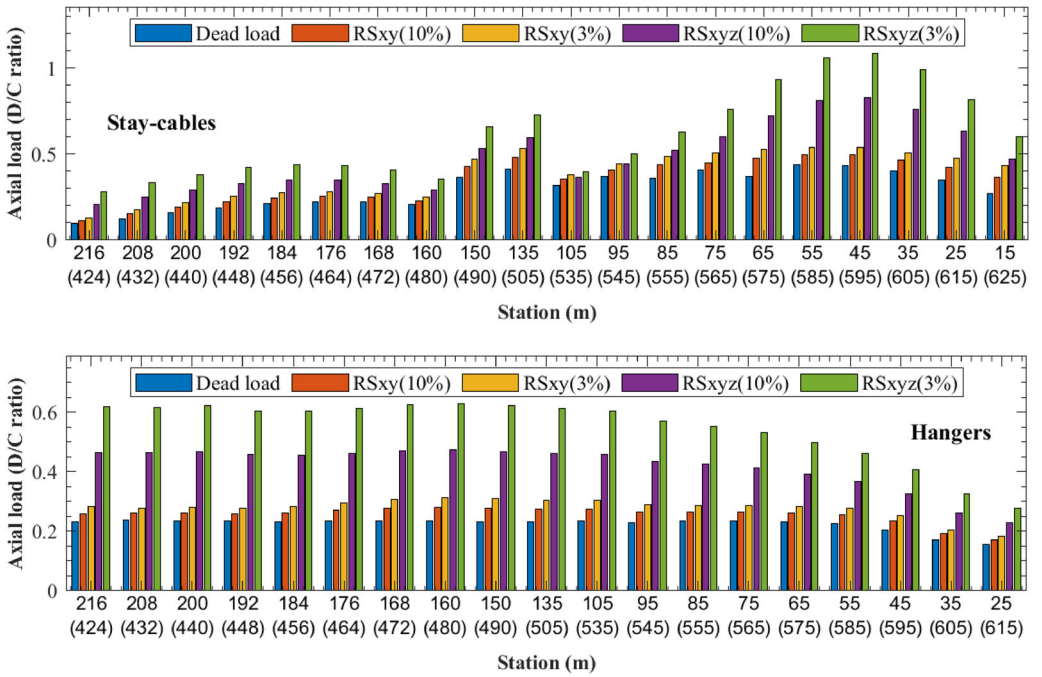

Figure 7. Axial forces of stay cables and hangers under considered load cases.

from horizontal response spectra were compared to the results of the three-component response spectra. The effects of the vertical seismic excitation are related to the vertical displacement and forces in the vertical direction, such as the axial force and moment about the major axis. According to Figure 8, the vertical displacement value of the middle of the deck under the horizontal response spectra is near to the value obtained from the dead load. However, the vertical component of the seismic load increases the displacement values of the bridge deck considerably, so that the maximum displacement is increased from the values of 0.555 m under the horizontal seismic load to 0.734 m under the three-component seismic load with a probability case of 3%. Nonetheless, lateral and torsional responses are not affected by the vertical seismic excitation. The sudden changes in the values occurred in stations 70 and 570 m, where the side arches are joined to the side deck, and the forces are distributed from side arches to the bridge deck. As it is observed from Figure 8, several responses of the bridge are more considerable under the seismic load, such as moment about a minor axis (especially in the middle of the main deck), torsion

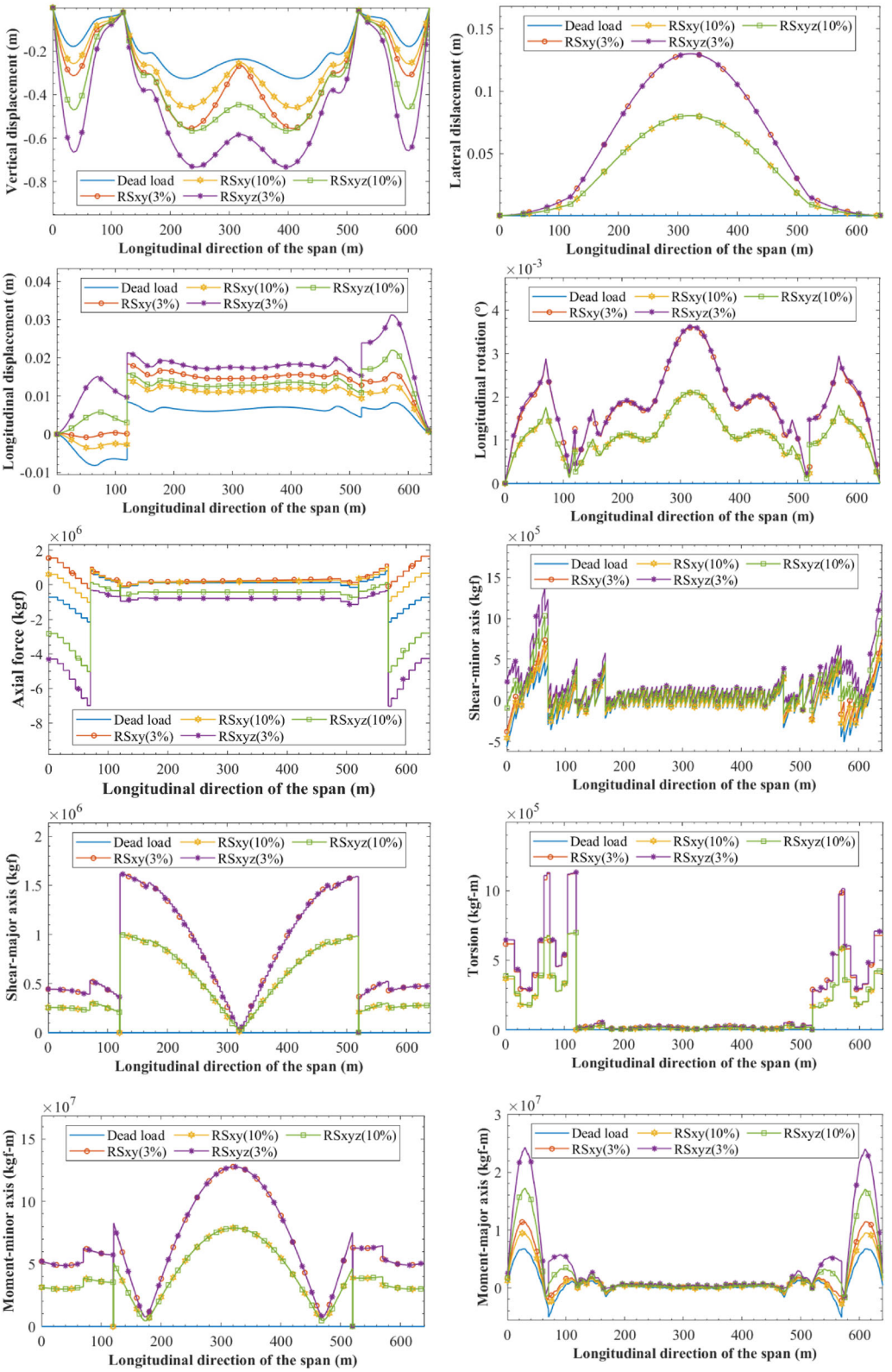

Figure 8. Responses of the bridge along layout-line under dead load, and multi-component seismic loading.

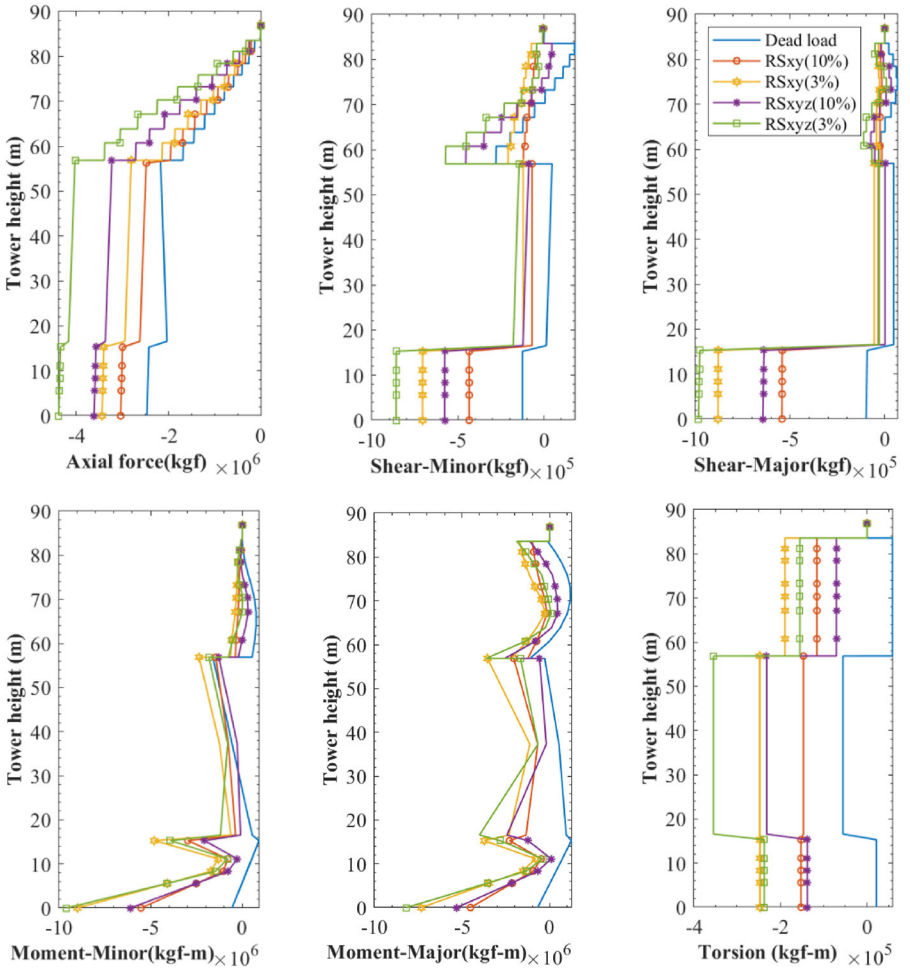

Figure 9. Responses of the bridge towers.

(especially inside decks), shear along the minor axis (connecting joints of main and side decks) and lateral displacements (the middle and quarter of the main deck). Likewise, several points of the bridge are more sensitive due to the abrupt changes in the values of the responses. These points are the connecting joints of the side deck and side arches, intersecting joints of towers and deck and the position of the connection between the main deck and the first hangers on each side.

4.1.4. Towers

In the cable-arch bridge, towers play a significant role in controlling the arch displacements further than supporting the deck and controlling its response. So, the responses of towers should be carefully monitored. For this purpose, the responses under the self-weight and seismic load cases are presented and compared according to Figure 9. It is evident from the figures that seismic loads intensify the moments in each direction. For the horizontal load case, the maximum axial force of the towers is related to the bent columns, and it is reduced in the tower's middle section (above the bent column); however, with the existence of the vertical component, the axial force is not considerably altered in the mentioned sections of the tower that means higher demand for

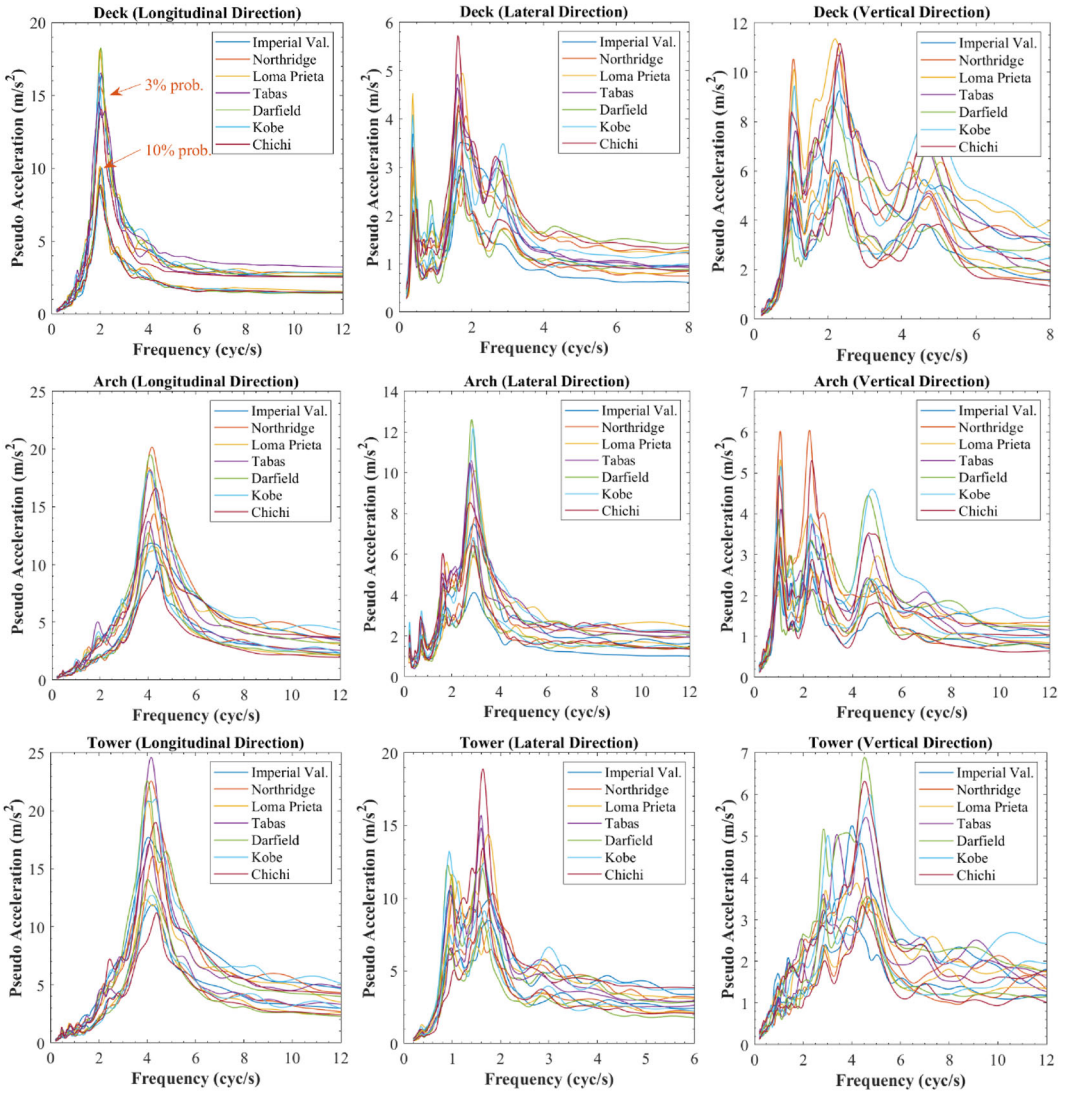

Figure 10. The spectral accelerations of the deck, arch, and tower considering the 10 and 3% hazard probability.

this section. The bent columns are very crucial parts of towers since they withstand the maximum forces and moments of the whole tower. This matter can be seen in Figure 9.

4.2. Time-history analysis

To assess the seismic performance of the bridge, the pseudo accelerations of different parts of the bridge are presented in Figure 10. According to these figures, the seismic ground motion records are the same as those given in Table 2. The middle of the bridge deck, towers' peak, and the arch crown are considered as measurement points to obtain responses. According to Figure 10, in some of the responses, such as the vertical directions of the deck and arch, the maximum accelerations occur within the initial modes. In some cases, the maximum accelerations are related to the same frequencies. For example, both deck and arch are subjected to maximum acceleration vertically in the frequency range of 1–2 cycle/s. Likewise, both arch and tower are subjected to maximum longitudinal acceleration in 4 cycles/s frequency. Several parts of the bridge in each

Table 6. Relative responses of the bridge subjected to earthquake records considering hazard probabilities.

	Displacement (cm)									Acceleration (m/s^2)								
	Arch crown			Tower			Center of deck			Arch crown			Tower			Center of deck		
Event Name	*Ux*	*Uy*	*Uz*	*Ux*	*Uy*	*Uz*	*Ux*	*Uy*	*Uz*	Long.	Tra.	Vert.	Long.	Tra.	Vert.	Long.	Tra.	Vert.
Hazard of 10% exceeding probability in 100 years																		
Imp. V.	0.43	12.5	−15.21	12.10	4.89	−2.29	1.48	5.06	−20.68	2.13	0.95	0.64	2.45	2.03	0.75	1.40	0.59	1.42
Northridge	0.28	9.27	−15.35	12.12	4.16	−2.31	1.57	5.74	−19.80	1.81	1.29	0.66	2.17	1.74	0.68	1.37	0.64	1.27
Loma P.	0.38	9.05	−15.17	12.24	3.85	−2.27	1.51	7.82	−20.07	1.70	1.03	0.71	2.30	1.54	0.87	1.49	0.74	1.68
Tabas	0.49	10.75	−15.13	12.28	4.60	−2.35	2.60	5.78	−20.78	2.22	1.75	0.70	2.25	2.47	0.83	2.11	0.85	1.64
Darfield	0.48	8.83	−14.99	12.18	4.17	−2.26	1.50	5.95	−20.37	1.91	0.95	0.60	1.99	1.64	0.88	1.31	0.83	1.48
Kobe	0.44	14.72	−15.07	12.42	4.44	−2.31	1.45	6.72	−20.45	1.69	1.14	0.73	1.95	2.00	0.97	1.41	0.67	1.98
Chichi	0.33	9.78	−15.41	12.29	3.99	−2.29	1.50	6.31	−19.62	1.67	1.33	0.56	2.10	1.94	0.48	1.42	0.7	1.16
Average	0.4	10.7	−15.19	12.23	4.3	−2.3	1.66	6.2	−20.25	1.88	1.21	0.66	2.17	1.91	0.78	1.5	0.72	1.52
Stand. Dev.	0.08	2.18	0.15	0.11	0.36	0.03	0.42	0.88	0.44	0.22	0.28	0.06	0.18	0.31	0.16	0.27	0.1	0.28
Hazard of 3% exceeding probability in 100 years																		
Imp. V.	0.62	21.32	−15.72	12.66	7.35	−2.42	2.07	9.24	−21.85	3.24	1.48	0.99	3.78	3.15	1.03	2.51	0.93	2.14
Northridge	0.47	16.13	−16.59	12.68	6.83	−2.43	2.32	10.10	−21.78	3.23	1.81	1.31	3.79	2.67	0.93	2.51	0.9	2.27
Loma P.	0.52	15.94	−16.08	12.59	5.82	−2.42	2.19	10.74	−22.10	2.54	1.83	0.93	2.86	2.73	1.24	2.62	1.15	3.71
Tabas	0.49	16.28	−16.07	12.87	5.07	−2.46	2.26	8.49	−22.42	2.70	1.76	1.09	3.29	2.7	1.05	2.22	0.85	2.93
Darfield	0.54	15.35	−15.79	12.57	7.46	−2.46	2.15	9.59	−21.92	2.78	1.77	1.25	2.99	2.77	1.73	2.57	1.34	1.93
Kobe	0.69	21.06	−16.38	12.96	7.19	−2.44	2.12	11.48	−21.90	2.87	1.79	1.34	3.62	3.25	1.27	2.68	0.91	2.49
Chichi	0.45	17.68	−16.24	12.74	5.75	−2.35	2.10	10.23	−21.67	3.14	2.13	0.88	3.63	3.63	0.9	2.48	0.97	1.85
Average	0.54	17.68	−16.12	12.72	6.5	−2.43	2.17	9.98	−21.95	2.93	1.8	1.11	3.42	2.99	1.16	2.51	1.01	2.47
Stand. Dev.	0.09	2.5	0.31	0.14	0.94	0.04	0.09	0.99	0.25	0.28	0.19	0.19	0.38	0.37	0.29	0.15	0.18	0.66

direction were affected with higher responses, more than the other parts. For the vertical and longitudinal direction, the deck and tower were affected more than the other section, respectively. As presented in Table 6, the accelerations and displacements of various parts were achieved from different seismic excitations for comparison. According to ASCE/SEI-7 (2016), the average response due to considered seismic records was considered as the bridge response in each direction. The *x*, *y*, *z* directions are according to the coordinate axis presented in Figure 2.

Neglecting the vertical component of the seismic records can cause remarkable effects on the structures (Di Sarno, Elnashai, and Manfredi 2011). It is obvious in Figure 11 that the axial load in the bridge is affected remarkably considering the vertical excitation. This figure proves the importance of the three-component earthquake excitation and the effects of its vertical component, which should be considered in seismic analysis of the structures.

4.3. Load-bearing capacity of the bridge using the pushover analysis

Bridges are the important types of structures which should resist various kinds of loads. The load-bearing capacity of the bridges is very important regarding the design of these structures. Among different structural elements, bent columns are the important parts of the bridge in resisting the lateral seismic load, and investigating the failure limit of the bridge; therefore, the behavior of the isolated bent columns with the equivalent loads from the bridge should be monitored under pushover analysis until the plastic hinges are generated. By considering the different load cases, the plastic hinges and capacity curves of each bent-column in each direction are presented in Figure 12. It is seen that in the probability case of 3%, the change in target displacement leads the bridge to exceed the collapse limit. The color of generated plastic hinges on the piers shows the performance level of the structure under the considered load cases.

The failure limit and the maximum bearable input in seismic vulnerability assessment can also be identified using time-history analyses, amplifying the input up to identify the average PGA associated with the failure/collapse (Domaneschi et al. 2021; Marasco et al. 2021). However, more analysis such as Incremental Dynamic Analysis (IDA) and fragility analysis is also required in

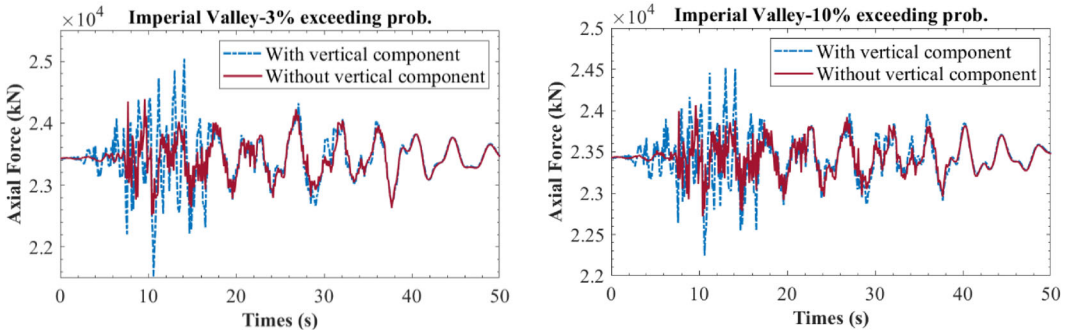

Figure 11. The effect of the vertical excitation of a typical seismic record on the axial force is each section of the arch.

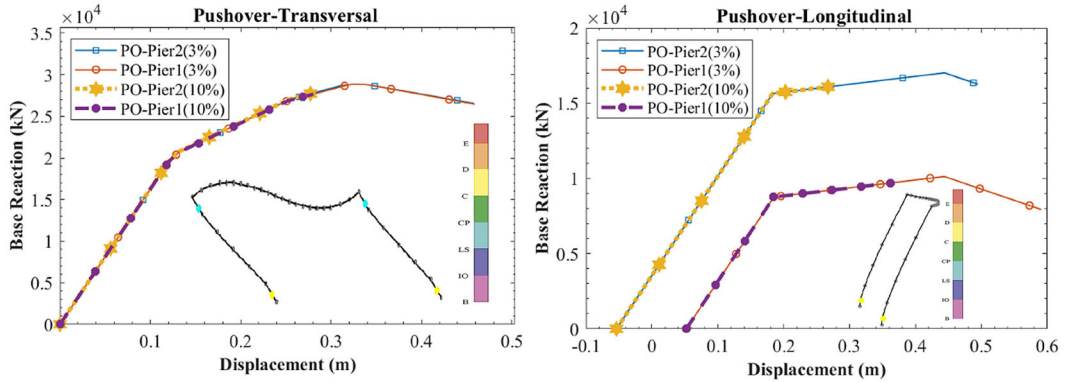

Figure 12. Pushover curves of the isolated bent columns with equivalent load.

future studies in which the scaled records should be applied on the whole bridge instead of isolated bent-columns to find the collapse limit in the bridge.

5. Conclusions

In this study, a finite element modeling of a hybrid cable-arch bridge and its seismic performance were presented using the response spectrum analysis under two hazard probabilities (3 and 10% exceeding probability in 100 years), time-history analysis with seismic ground motions and pushover analysis. Effects of the vertical component of the response spectrum and seismic records were also considered. The responses of the bridge components were investigated under different load cases, and the following results were obtained for the case study bridge:

1. There was a significant difference between the seismic responses of the studied bridge under two seismic hazard probabilities, and the maximum responses occurred in the case of 3% exceeding probability in 100 years. Thus, for the seismic safety of the bridge, both probabilities need to be checked.
2. By applying the vertical component to the horizontal seismic load (three-component seismic load), the responses were increased, especially in the vertical direction. Thus, the most severe load case was the case of the three-component seismic excitations with the probability of 3%.
3. By using pushover analysis and the capacity curves of bent columns, the nonlinear behavior of bridge piers was investigated, and their vulnerability was proved, especially in the transverse direction.

4. According to the responses, a special seismic consideration should be provided for the different parts of the bridge that is vulnerable under seismic loads, such as connecting joints of side deck and side arches, the intersecting joints of the deck and towers, and the position of the connection between the main deck and the first hangers in each side.
5. The behavioral investigation of bent columns and stay-cables under seismic loads is very important in this type of bridge. Bent columns are the important components of the bridge in resisting the lateral seismic load. Also, stay cables play a key role in supporting the main arch in this kind of bridge since the longitudinal and lateral displacements of the arch are controlled by these cables, which provide the stability for the arch and the whole bridge.

Future studies can include suggestions such as the seismic fragility analysis of bridge systems, investigating the stability and feasibility of larger spans using energy dissipation systems, etc.

Disclosure statement

No potential conflict of interest was reported by the author.

ORCID

Salar Farahmand-Tabar http://orcid.org/0000-0002-7520-5452
Majid Barghian http://orcid.org/0000-0002-8765-7958

References

Aghabeigi, P., and S. Farahmand-Tabar. 2021. Seismic vulnerability assessment and retrofitting of historic masonry building of Malek Timche in Tabriz Grand Bazaar. *Engineering Structures* 240:112418. doi:10.1016/j.engstruct.2021.112418.

American Association of State Highway and Transportation Officials (AASHTO). 2012. LRFD bridge design specifications, customary U.S. units. Washington, DC.

Bamer, F., and B. Markert. 2017. An efficient response identification strategy for nonlinear structures subject to nonstationary generated seismic excitations. *Mechanics Based Design of Structures and Machines* 45 (3):313–30. doi:10.1080/15397734.2017.1317269.

Cassese, P., M. T. De Risi, and G. M. Verderame. 2020. Seismic assessment of existing hollow circular reinforced concrete bridge piers. *Journal of Earthquake Engineering* 24 (10):1566–601. doi:10.1080/13632469.2018.1471430.

Di Sarno, L., A. S. Elnashai, and G. Manfredi. 2011. Assessment of RC columns subjected to horizontal and vertical ground motions recorded during the 2009 L'Aquila (Italy) earthquake. *Engineering Structures* 33 (5):1514–35. doi:10.1016/j.engstruct.2011.01.023.

Domaneschi, M., A. Zamani Noori, M. V. Pietropinto, and G. P. Cimellaro. 2021. Seismic vulnerability assessment of existing school buildings. *Computers & Structures* 248:106522. doi:10.1016/j.compstruc.2021.106522.

Dos Santos, R. C., A. P. C. Larocca, J. O. de Araújo Neto, A. C. B. Barbosa, and J. V. M. Oliveira. 2019. Detection of a curved bridge deck vibration using robotic total stations for structural health monitoring. *Journal of Civil Structural Health Monitoring* 9:63–76. doi:10.1007/s13349-019-00322-1.

Elnashai, A. S., and L. Di Sarno. 2008. *Fundamentals of earthquake engineering*. UK: Wiley and Sons.

Falamarz-Sheikhabadi, M. R., and A. Zerva. 2017. Analytical seismic assessment of a tall long-span curved reinforced-concrete bridge. Part II: Structural response. *Journal of Earthquake Engineering* 21 (8):1335–64. doi:10.1080/13632469.2016.1211566.

Farahmand-Tabar, S., and M. Barghian. 2021. Seismic assessment of a cable-stayed arch bridge under three-component orthotropic earthquake excitation. *Advances in Structural Engineering* 24 (2):227–42. doi:10.1177/1369433220948756.

Farahmand-Tabar, S., and M. Bargian. 2020. Formulating the optimum parameters of modified hanger system in the cable-arch bridge to restrain force fluctuation and overstressing problems. *Journal of the Brazilian Society of Mechanical Sciences and Engineering* 42:453. doi:10.1007/s40430-020-02513-0.

Farahmand-Tabar, S., and M. Bargian. 2020. Response control of cable-stayed arch bridge using modified hanger system. *Journal of Vibration and Control* 26 (23–24):2316–28. doi:10.1177/1077546320921635.

Farahmand-Tabar, S., M. Bargian, and M. Vahabzadeh. 2019. Investigation of the progressive collapse in a suspension bridge under the Explosive Load. *International Journal of Steel Structures* 19 (6):2039–50. doi:10.1007/s13296-019-00263-x.

Geradin, M., E. J. Sapountzakis, and E. V. Zahariev. 2017. Dynamics of structures subject to seismic excitations. *Mechanics Based Design of Structures and Machines* 45 (3):281. doi:10.1080/15397734.2017.1323643.

Hancock, J., J. Watson-Lamprey, N. A. Abrahamson, et al. 2006. An improved method of matching response spectra of recorded earthquake ground motion using wavelets. *Journal of Earthquake Engineering* 10 (sup001):67–89. doi:10.1080/13632460609350629.

Hao, Q., S. Jufeng, and H. Pingming. 2017. Study on dynamic characteristics and seismic response of the extradosed cable-stayed bridge with single pylon and single cable plane. *Journal of Civil Structural Health Monitoring* 7:589–99. doi:10.1007/s13349-017-0243-6.

He, G. J., Z. Q. Zou, Y. Q. Ni, and J. M. Ko. 2009. Seismic response analysis of multi-span cable-stayed bridge. *Key Engineering Materials* 400:737–42.

Huang, C., and S. Huang. 2020. Predicting capacity model and seismic fragility estimation for RC bridge based on artificial neural network. *Structures* 27:1930–9. doi:10.1016/j.istruc.2020.07.063.

Jin, M., B. Wang, Z. Feng, and X. Wang. 2012. Seismic response analysis of long Span Cable-stayed Bridge. *Applied Mechanics and Materials* 204:1992–6.

Kang, H. J., Y. Y. Zhao, and H. P. Zhu. 2014. Analytical and experimental dynamic behavior of a new type of cable-arch bridge. *Journal of Constructional Steel Research* 101:385–94. doi:10.1016/j.jcsr.2014.06.005.

Kang, H. J., Y. Y. Zhao, H. P. Zhu, and Y. X. Jin. 2013. Static behavior of a new type of cable-arch bridge. *Journal of Constructional Steel Research* 81:1–10. doi:10.1016/j.jcsr.2012.10.010.

Klein, P., and M. Yamout. 2003. Cable-stayed arch bridges, Putrajaya, Kuala Lumpur, Malaysia. *Structural Engineering International* 13 (3):196–9. doi:10.2749/101686603777964586.

Li, J. B., and J. Ge. 2005. Seismic analysis of a 5-span half-through CFST arch bridge. *World Earthquake Engineering* 25 (3):110–5.

Li, J., and J. Li. 2004. An efficient response spectrum analysis of structures under multi-support seismic excitations. *Proceedings of the 13th World Conference on Earthquake Engineering*, Vancouver, Canada.

Liu, X., L. Jiang, P. Xiang, Z. Lai, L. Liu, S. Cao, and W. Zhou. 2021. Probability analysis of train-bridge coupled system considering track irregularities and parameter uncertainty. *Mechanics Based Design of Structures and Machines* 1–18. doi:10.1080/15397734.2021.1911665.

Li, S., B. Wei, H. Tan, C. Li, and X. Zhao. 2021. Equivalence of friction and viscous damping in a spring-friction system with concave friction distribution. *Journal of Testing and Evaluation* 49 (1):20190885–395. doi:10.1520/JTE20190885.

Luo, S., X. Wang, T. Wang, and X. Gui. 2005. Considerations and study of innovative techniques for long-span cable-stayed arch bridge. *Bridge Construction* 6:31–3. (in Chinese)

Ma, J., Y. J. Chen, and L. P. Liu. 2011. Nonlinear seismic response analysis of half through CFST arch bridge under 3-D earthquake waves. *Key Engineering Materials* 456:67–76.

Marasco, S., A. Zamani Noori, M. Domaneschi, and G. P. Cimellaro. 2021. Seismic vulnerability assessment indices for buildings: Proposals, comparisons and methodologies at collapse limit states. *International Journal of Disaster Risk Reduction* 63 (102466):102466. doi:10.1016/j.ijdrr.2021.102466.

Marefat, M. S., M. Yazdani, and M. Jafari. 2019. Seismic assessment of small to medium spans plain concrete arch bridges. *European Journal of Environmental and Civil Engineering* 23 (7):894–915. doi:10.1080/19648189.2017.1320589.

Nakamura, S., H. Tanaka, and K. Kato. 2009. Static analysis of cable-stayed bridge with CFT arch ribs. *Journal of Constructional Steel Research* 65 (4):776–83. doi:10.1016/j.jcsr.2008.05.005.

Narayana Murthy, T., and G. R. Patil. 2015. Effect of vertical ground motion on reinforced concrete structures. *IOSR Journal of Mechanical and Civil Engineering* 2:33–9.

Niu, Y. Z., W. J. Guo, G. L. Li, and R. X. Sun. 2014. The seismic response analysis of long-span cable-stayed bridge. *Applied Mechanics and Materials* 501:1364–7.

Rahai, A. 2004. Effect of earthquake vertical motion on RC bridge piers. In The 13th world conference on earthquake engineering, Vancouver, BC, Canada, 1–6 August.

SeismoMatch. 2020. A computer program for spectrum matching of earthquake records. Available from https://seismosoft.com.

Taghinia, A., A. Vasseghi, M. Khanmohammadi, et al. 2021. Development of Seismic Fragility Functions for Typical Iranian Multi-Span RC Bridges with Deficient Cap Beam–Column Joint. *International Journal of Civil Engineering* 20:305–21. doi:10.1007/s40999-021-00661-5.

Todorov, B., and A. Billah. 2021. Seismic fragility and damage assessment of reinforced concrete bridge pier under long-duration, near-fault, and far-field ground motions. *Structures* 31:671–85. doi:10.1016/j.istruc.2021.02.019.

Wang, W., W. Yan, L. Deng, and H. Kang. 2015. Dynamic analysis of a cable-stayed concrete-filled steel tube arch bridge under vehicle loading. *Journal of Bridge Engineering* 20 (5):04014082. doi:10.1061/(ASCE)BE.1943-5592.0000675.

Wang, X. W., and A. J. Ye. 2011. Computational mode number research in seismic response spectrum Analysis of Long-Span Cable-Stayed Bridge. *Journal of Structural Engineers* 27 (4):84–90.

Wang, C., J. Zhao, L. Zhu, and Y. Bao. 2016. Effects of vertical excitation on the seismic performance of a seismically isolated bridge with sliding friction bearings. *Earthquake Engineering and Engineering Vibration* 15 (1):187–96. doi:10.1007/s11803-016-0315-3.

Wei, B., Z. Hu, X. He, and L. Jiang. 2020. Evaluation of optimal ground motion intensity measures and seismic fragility analysis of a multi-pylon cable-stayed bridge with super-high piers in Mountainous Areas. *Soil Dynamics and Earthquake Engineering* 129 (105945):105945. doi:10.1016/j.soildyn.2019.105945.

Wei, B., W. H. Wang, P. Wang, T. H. Yang, L. Z. Jiang, and T. Wang. 2020. Seismic responses of a high-speed railway (HSR) bridge and track simulation under longitudinal earthquakes. *Journal of Earthquake Engineering* 26 (9):4449–4470. doi:10.1080/13632469.2020.1832937.

Yang, H., X. Yin, H. Hao, and K. Bi. 2016. Theoretical investigation of bridge seismic responses with pounding under near-fault vertical ground motions. *Advances in Structural Engineering* 18 (4):453–68. doi:10.1260/1369-4332.18.4.45.

Yu, J., L. Jiang, W. Zhou, X. Liu, Z. Lai, and Y. Feng. 2020. Study on the dynamic response correction factor of a coupled high-speed train–track–bridge system under near-fault earthquakes. *Mechanics Based Design of Structures and Machines* 50 (9):3303–21. doi:10.1080/15397734.2020.1803753.

Zhang, Y., L. Jiang, W. Zhou, S. Liu, X. Liu, L. Wu, T. Zhou, and G. Shao. 2021. Study of resonance condition of railway bridge subjected to train loads with a four-beam system. *Mechanics Based Design of Structures and Machines* 51 (3):1468–88. doi:10.1080/15397734.2021.1873147.

Zhao, Y. Y., X. Z. Yang, and H. J. Kang. 2005. Analysis of dynamic characteristics for cable-stayed arch bridge. *Highway* 11:36–40. (in Chinese).

Zheng, L., L. Jiang, Y. Feng, X. Liu, Z. Lai, and W. Zhou. 2020. Effects of foundation settlement on comfort of riding on high-speed train-track-bridge coupled systems. *Mechanics Based Design of Structures and Machines* 50 (8):2760–778. doi:10.1080/15397734.2020.1784204.